# Critical properties of unlimited gliding: Unexpected flocking behavior driven by the exchange of information

Marta Bigus-Kwiatkowska, Agata Fronczak, and Piotr Fronczak
*Faculty of Physics, Warsaw University of Technology, Koszykowa 75, PL-00-662 Warsaw, Poland*

(Received 1 December 2017; revised manuscript received 4 March 2018; published 28 March 2018)

Inspired by albatrosses that use thermal lifts to fly across oceans we develop a simple model of gliders that serves us to study theoretical limitations of unlimited exploration of the Earth. Our studies, grounded in physical theory of continuous percolation and biased random walks, allow us to identify a variety of percolation transitions, which are understood as providing potentially unlimited movement through a space in a specified direction. We discover an unexpected phenomenon of self-organization of gliders in clusters, which resembles the flock organization of birds. This self-organization is intriguing, as it occurs thanks to exchange of information only and without any particular rules that could favor the clustering of the gliders (in contrast to the causes well known in literature, like, for example, attractive forces used in the Vicsek-type models or fitness functions used in evolutionary computation).

DOI: 10.1103/PhysRevE.97.032139

## I. INTRODUCTION

Recent advances in technology have made it possible to create unmanned aerial vehicles (UAVs), that is, aircraft without a human pilot aboard, commonly known as drones [1]. Potential applications of such aircraft, including terrain exploration, surveillance, coast control, and fire detection, have stirred the imagination of many engineers and scientists [2]. One of the most important problems with these applications is the short endurance of UAVs. Even ultralight sophisticated drones must land to refuel or recharge batteries. To overcome this problem, engineers have constructed UAV gliders [3], inspired by species of birds able to fly long distances without flapping their wings.

UAV gliders use atmospheric energy in its various forms to soar for extended periods [4]. Just as albatrosses or vultures use thermal lifts (vertical movements of the atmosphere) and updrafts to reach high altitudes without muscle effort [5], UAVs benefit from thermals. Modern gliders exploit specialized soaring algorithms to detect the present position of a thermal and predict its future position [6,7]. These algorithms enable gliders to ride thermals continuously using a sequence of alternately climbing and gliding on the search for the next thermal. A substantial and rapidly growing body of literature on engineering issues addresses the design of UAV gliders, especially their aerodynamics [8], communication protocols [10], energy consumption [9], and thermal identification [11]. However, along with technical problems, many theoretical aspects of long-lasting glides have emerged.

For example, it would not be possible for UAVs to cover long distance without a virtually connected path of thermals along which the glider could travel. This problem is closely related to the concept of percolation, which has been thoroughly explored since the late 1950s [12], bringing new understanding and techniques to a broad range of topics in physics, materials science, complex networks, epidemiology, and other fields (see review in [13]).

In the context of thermal glides, a special branch of percolation theory known as continuum percolation seems to be the most attractive. This concept was developed by Gilbert in 1961 [14] to describe a network of transceivers scattered randomly in a plane, each of which communicating with other within a fixed distance. It has been shown that some control parameters (e.g., the density of transceivers or their broadcast range) have a critical value known as the percolation threshold. Above this threshold, a packet of information can be delivered successfully from the sender of a message to its receiver through the network of transceivers. By analogy, one can expect that a UAV glider can travel through scattered thermals covering long distances. The problem seems to be slightly complicated by the fact that the thermals, in contrast to fixed transceivers, are temporary moving objects. In addition, identifying a thermal position is not a trivial task, whereas the electromagnetic wave reaches a receiver easily. This paper discusses the critical properties of a continuum percolation system of thermals and efficient thermal riding.

Another interesting concept that becomes important, especially when a large number of UAVs interact with each other, is the phenomenon of self-organization [15], which describes the ability of a system to spontaneously arrange its elements into complex yet coordinated patterns without specific interference from the outside. Recently, these systems have become of great interest to the mathematical [16], physical [17,18], and biological sciences [19], with insect swarm, fish schools, and bird flocks inspiring engineers who are developing autonomous robotic swarms [20]. It has been proven that cooperative missions with multiple vehicles enable faster detection and more efficient exploitation of thermals [21,22]. Below, we demonstrate that a system of cooperating gliders is characterized by certain critical properties. Specifically, there exist critical values of some system parameters (i.e., the number of gliders and the range of their transmitters) that separate the phase of unconstrained flow from the phase in which each glider is pinned to the nearest thermal. Furthermore, we show that gliders can self-organize in clusters resembling the flock organization of birds. Interestingly, these clusters emerge without a direct force that attracts the gliders toward one another (like the force typical in Vicsek models of swarm formation [17]).

The paper is organized as follows. First, we develop a model of a glider that explores the neighboring area in a random walk manner, searching for potential thermals. Then, we describe the limits of long-distance rides, identifying the existence of a critical density in thermals and their critical velocity. We present the concept of cooperating gliders. We show that such cooperation can improve the efficiency of flight, demonstrate the effect of clustering among gliders, and investigate the critical properties of such clustering. Finally we present concluding remarks and briefly discuss possible extensions of the model.

## II. GLIDER MODEL

Because the present paper focuses on the general properties of percolation and self-organization phenomena, our model of gliders and thermals contemplates only what we deem essential for such a focus. In particular, each thermal is defined by a vertical cylinder of radius $R$ and height $H$, meaning that we disregard any differences in local air temperature and the resulting fluctuations in vertical wind velocity. A number $N_t$ of such thermals are distributed randomly in the area $L \times L$ with density $\rho = N_t/L^2$ and periodic boundary conditions. To further simplify implementation, we assume that the thermals do not move. However, to keep the model sufficiently realistic, we introduce a type of memory $t_m$ of a glider, which is a time since its last visit for which the glider remembers the position of a given thermal. This means that we assume that after $t_m$ a thermal could move sufficiently far from its known position to be identified easily by a glider and its location is unreliable.

We define a glider as a material point that can move in three dimensions at constant speed with the following rules.

(1) Inside the thermal the vertical speed of the glider becomes $v_z = v_\uparrow > 0$, while the horizontal speed $\vec{v_h} = [v_x, v_y]$ is set to zero. This means that when the glider finds a thermal, the drone is lifted by warm air until it reaches height $H$. Again, assuming a zero turning radius, we simplify the real aerodynamic properties of the gliders.

(2) Then, the glider begins exploring the sky, searching for a new thermal. It glides with a given $v_h > 0$ and falls with $v_z = v_\downarrow < 0$. The exploration is imitated by a biased random walk. A bias is introduced to impose the specific direction of the flight, let us say along the $x$ axis. It is implemented by an angle of flight drawn from the Gaussian distribution $\mathcal{N}(0,\sigma)$ every time unit $\Delta t$.

(3) When the glider finds a thermal (i.e., when it is less than $R$ from the thermal), it flies up towards its center.

(4) To ensure that the glider does not fall, it must return directly to the nearest known thermal, if its altitude

$$z < \max(H/2, H + v_\downarrow t_m/2). \tag{1}$$

This means that the glider will switch from the exploration phase to the return phase, choosing the nearest of the memorized thermals and flying toward it along a straight line.

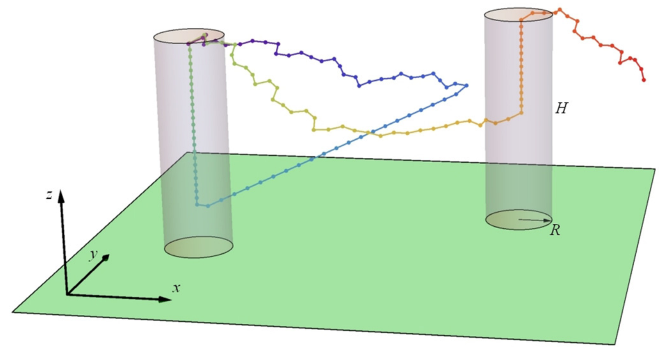


FIG. 1. A typical flight performed by a glider. Time is visualized by the colors of the rainbow. Two thermals are visible. The path begins at the top of the left thermal. After an unsuccessful search for the next thermal, the glider returns directly to the left thermal and gains altitude. During the next exploration, a new thermal is found. The glider exploits its lift energy and continues the flight in the right direction.

(5) To take into account the cooperation between $N_g$ gliders, we assume that they can exchange information about known thermals. When the glider finds a thermal, it broadcasts a message about the discovered thermal's location for the gliders within its transmitter range $R_I$.

Figure 1 and the movie `example1.avi` in the Supplemental Material present the typical behavior of a glider [23]. Table I provides a summary of the parameters used in the numerical simulations.

## III. PERCOLATION IN THERMAL GLIDING

In the context of gliders, we define percolation as the possibility of unlimited movement through a space in a specified direction. Thus, to describe the critical point accurately, we use the following order parameter:

$$\langle v_x \rangle = \frac{\sum_{i=1}^{N_g} \langle v_x^{(i)} \rangle}{N_g}, \tag{2}$$

where $\langle v_x^{(i)} \rangle$ is the speed of the $i$th glider in $x$ direction averaged over a sufficiently long time $t$. For the density of

TABLE I. Summary of the parameters used in the simulations.

| Parameter | Label | Value | Unit |
|---|---|---|---|
| Linear size of the system | $L$ | 200 | km |
| Height of thermal | $H$ | 10 | km |
| Radius of thermal | $R$ | 1 | km |
| Speed of climb | $v_\uparrow$ | 0.2 | km/min |
| Falling speed | $v_\downarrow$ | $-0.1$ | km/min |
| Horizontal speed | $v_h$ | 1 | km/min |
| Angle standard deviation | $\sigma$ | $\pi/4$ | rad |
| Time between turning | $\Delta t$ | 1 | min |
| Time step of simulation | Time step | 0.1 | min |
| Number of thermals | $N_t$ | $40 \div 40\,000$ | |
| Number of gliders | $N_g$ | $10 \div 100$ | |
| Memory | $t_m$ | $0 \div 1000$ | min |
| Radius of information | $R_I$ | $0 \div 100$ | km |

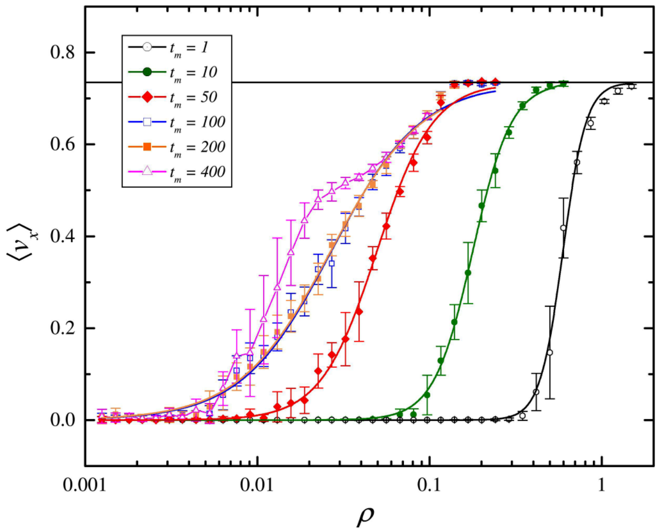


FIG. 2. The order parameter $\langle v_x \rangle$ vs $\rho$ for different values of memory $t_m$ of gliders. The values are averaged over 100 different simulations and over time $t = 50\,000$. The system parameters are $L = 200$, $H = 10$, $R = 1$, $v_\uparrow = 0.2$, $v_\downarrow = -0.1$, and $\sigma = \pi/4$. The continuous lines represent fit by a logistic curve.

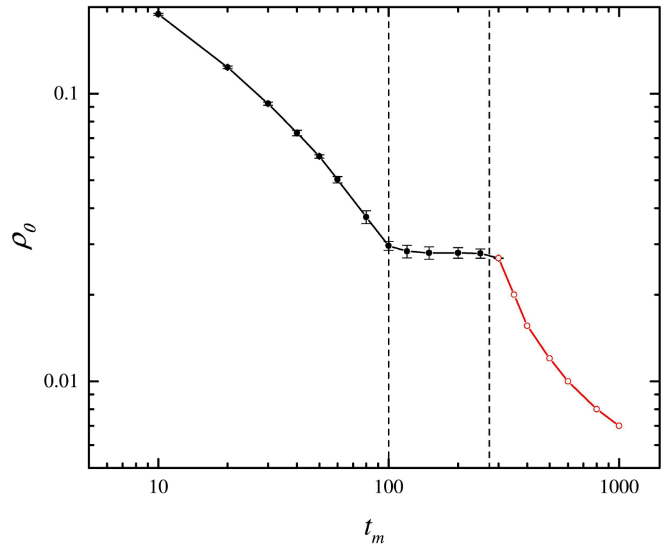


FIG. 3. A midpoint $\rho_0$ of the logistic curves used in Fig. 2 as a function of memory $t_m$ of gliders. The vertical lines separate three different regions of behavior of $\rho_0$. The points marked in red are found using the condition $\langle v_x \rangle(\rho) = \langle v_x \rangle_{\max}/2$ (they cannot be found from the fitting). The parameters used are the same as in Fig. 2.

thermals $\rho < \rho_c$, each glider performs an infinite cycle of the unsuccessful search for the next thermal and the return flight to its original thermal. Thus, its $\langle v_x^{(i)} \rangle = 0$ and $\langle v_x \rangle = 0$. Otherwise, for $\rho > \rho_c$, $\langle v_x \rangle \to v_{\max}$, where $v_{\max}$ is a constant larger than zero, and the gliders will gradually discover new thermals and move along the $x$ direction. Therefore, a phase transition occurs at $\rho = \rho_C$ and $\rho_C$ is the minimal density of thermals that allow unlimited exploration of space. Figure 2 presents a typical behavior of the order parameter for various values of memory $t_m$.

The maximal value of the order parameter can be derived from the average $x$-axis projection of the horizontal speed $v_h$:

$$\langle v_x \rangle_{\max} = v_h \langle \cos|\theta| \rangle, \tag{3}$$

where $\theta \sim \mathcal{N}(0,\sigma)$ is a Gaussian distributed horizontal angle of the flight. Expanding the cosine function into the Maclaurin series

$$\cos|\theta| = \sum_{n=0}^{\infty} \frac{(-1)^n \theta^{2n}}{(2n)!} \tag{4}$$

and using the known formula for the central absolute moments of the even order of the normal distribution

$$\mathbf{E}[\theta^p] = \sigma^p (p-1)!!, \tag{5}$$

one finally obtains

$$\langle v_x \rangle_{\max} = v_h e^{-\sigma^2/2}. \tag{6}$$

The horizontal line in Fig. 2 represents the maximal value of the order parameter for the standard deviation $\sigma = \pi/4$ and $v_h = 1$, the parameters used in the numerical simulations. The position of this value, calculated from Eq. (6), demonstrates perfect agreement with the simulations.

To quantify how the memory of the aircraft affects the location of the critical point, a logistic curve

$$\langle v_x \rangle = \frac{C}{\left(\frac{\rho}{\rho_0}\right)^{-a} + 1} \tag{7}$$

was used to fit the data and to determine the two curve parameters, $\rho_0$—the $\rho$ value of the sigmoid's midpoint—and $a$—the steepness of the curve. The curve's maximum value, $C$, is set by Eq. (6) at $C = \langle v_x \rangle_{\max}$. Figure 3 shows the behavior of the midpoint $\rho_0$ (related directly to $\rho_c$) as a function of memory $t_m$. Three different phases are visible therein. In the first phase the critical number of thermals allowing progressive flight decreases with $t_m$. This is reasonable, because the glider's memory reflects the stability of the thermals. The more stagnant the thermals are, the more extensive is the exploration of the terrain that is possible without returning to the thermal to gain altitude. This phase stops when further increase of the memory does not enable the glider to prolong the exploration. According to Eq. (1), the moment of turning toward the nearest known thermal depends on memory only for $t_m < -\frac{H}{v_\downarrow}$. For the parameters used in the numerical simulations, $H = 10$ and $v_\downarrow = -0.1$; the critical value of $t_m = 100$ is shown by the first vertical line in Fig. 3. For $t_m > -\frac{H}{v_\downarrow}$, the glider, despite the value of its memory, must complete the exploration phase at an altitude of $H/2$, since further drifting from the thermal, in the case of an unsuccessful search, may make it impossible to return to the last known thermal before landing.

The third phase shown in Fig. 3 is an artifact of the numerical simulations. It begins when the glider, after a full lap of the planet, still remembers the thermals it discovered during its previous exploration of the area, that is, when its memory $t_m > \frac{L}{\langle v_x \rangle_{\max}}$. Such atypical behavior is shown in Fig. 2 for $t_m = 400$, where a visible hump appears for intermediate values of the order parameter (in this case, the data points are not fitted by the

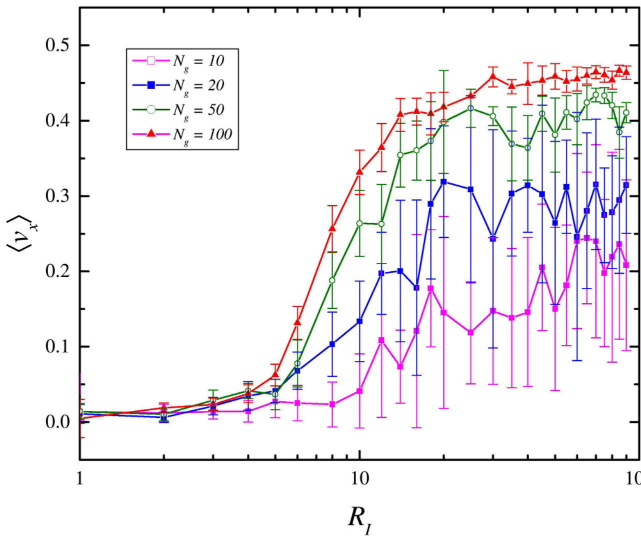


FIG. 4. The order parameter as a function of transmitter range $R_I$ of gliders for a given density of thermals $\rho = 0.02$ and memory $t_m = 50$ and for a different number of cooperating gliders $N_g$. The parameters used are the same as in Fig. 2.

logistic curve, but only connected by a line for better visibility). For the parameters used in the numerical simulations [$L = 200$ and $\langle v_x \rangle_{\max}$, which are calculated from Eq. (6)], Fig. 3 depicts the critical value of $t_m \approx 274$ by the second vertical line. The points to the right of this line are found using the condition $\langle v_x \rangle = \langle v_x \rangle_{\max}/2$, because the logistic model is then unsuitable.

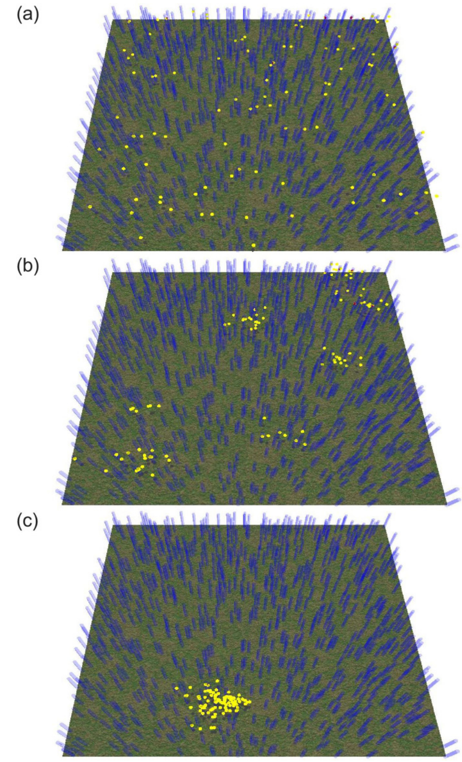


FIG. 5. Three snapshots of the simulation conducted for (a) $t = 1$, (b) $t = 100$, and (c) $t = 25\,000$. The gliders are represented by yellow dots, and the thermals are visible as vertical blue cylinders. The parameters used are $\rho = 0.02$, $N_g = 100$, $t_m = 50$, and $R_I = 20$.

## IV. SELF-ORGANIZATION OF COOPERATING GLIDERS

In this section, we present the effect of cooperation among gliders on improving the rate of their exploration.

The exchange of information among gliders about the positions of thermals enables a glider (during the return phase) to fly to a thermal that would remain undiscovered without the help of another UAV. In the best case, if the recently reported thermal is located on the right of the glider (with respect to the $x$ axis), the glider does not have to waste time returning to one of the thermals it discovered itself, which are usually located to the left of it. Then, its speed $v_x$ during the return phase is not only non-negative but even greater than during the exploration phase, as it now moves directly toward the thermal, rather than wandering randomly with bias. In Fig. 4, we compare the behavior of the order parameter as a function of the density of the thermals for solitary and cooperating gliders. As the figure shows, cooperation allows for efficient flight, even in the range previously unavailable to the gliders.

It is worth noting that there is a critical value of the transmitter range $R_I$, above which such an improvement is possible. The criticality of the control parameter is especially evident for large values of $N_g$. The above phenomenon is to some extent analogous to the Gilbert disk model [24] in the theory of continuous percolation. In that model, disks are scattered uniformly in the infinite plane $\mathbb{R}^2$ according to a homogeneous Poisson process, and at sufficiently high densities they can form infinite clusters allowing for, for example, unlimited information transmission. It is reasonable to expect that in the Gilbert model the position of the critical values of the two control parameters, the density of disks and their radii, should be negatively correlated (the larger the disks are, the fewer are needed to cover the space). In the model presented herein, the disks are represented by the areas of the transmission range of the UAVs. When increasing the number of gliders $N_g$, the analogy of the Gilbert model would lead one to expect that the critical value of the control parameter $R_I$ shown in Fig. 4 would decrease. However, this is not true, as Fig. 4 shows. The reason for this is not obvious and is related to the self-organization phenomena that occur in the model, which introduce heterogeneity to the system, making an analogy to the Gilbert model inappropriate. Below, we discuss this in detail.

Figure 5 shows three snapshots from the simulations made at time $t_1 = 0$, $t_2 > t_1$, and $t_3 > t_2$ (please see also the movie `example2.wmv` in the Supplemental Material [23]). At the beginning, the gliders (represented by yellow dots) are scattered uniformly in the plane. Over the course of the simulation, they gather, forming clusters that resemble flocks of birds. It is remarkable that such clustering is not caused by any attractive forces among the gliders nor by any penalty function favoring individuals flying faster—which is typical in evolutionary computation—but rather by mutual exchange of information. We believe that this is the most intriguing phenomenon observed in the model.

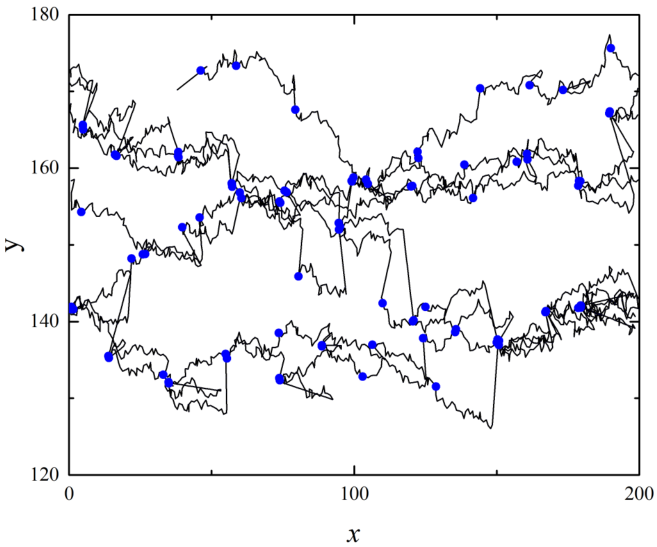


FIG. 6. The trajectory of a member of the flock presented in Fig. 5(c). Blue dots represent thermals visited by the glider.

At time $t_3$, only one flock of gliders is present and it seems to be a stable attractor of the system dynamics. If the total number of gliders is small, the cluster can break into smaller parts due to fluctuations in the local density of thermals. However, after some time, the global tendency to fly in a single flock prevails. Such continuous fragmentation and coagulation of the global cluster results in large fluctuations in the gliders' speeds: smaller clusters are characterized by a lower speed and larger clusters are characterized by a higher speed. This can be seen in Fig. 4, in which, for a small number of UAVs, $N_g$, the fluctuations are significant even for the large radius of transmission range $R_I$. For a large number of gliders, for example, $N_g = 100$ (the top curve in Fig. 4), the single cluster is stable despite the fluctuations in thermal density, and the fluctuations of the order parameter vanish with $R_I$. Please note that when the gliders form a flock their flight path can still vary. Figure 6 shows the trajectory of a single member of the flock. This trajectory does not pass through the same set of thermals. The flock still can explore the whole available area.

To quantitatively describe the phenomenon of clustering we use Ripley's statistics, a spatial analysis method used to detect deviations from spatial homogeneity [25]. It has been widely used in demography [26], ecology [27], biophysics [28], and neurology [29]. Ripley's K-function estimator is defined as follows:

$$K(r) = \frac{\lambda^{-1}}{N_g}\sum_{i=1}^{N_g} n_i(r), \tag{8}$$

where $n_i(r)$ is the number of points within a distance $r$ of another point $i$ and $\lambda$ is the average density of points (here, $\lambda = N_g/L^2$). Because for a homogeneous Poisson process $K(r) = \pi r^2$ for all $r$, in practice, it is easier to study the function

$$H(r) = \sqrt{K(r)/\pi} - r, \tag{9}$$

which for a homogeneous Poisson process should be equal to zero for all $r$. A positive value of $H(r)$ indicates clustering over that spatial scale whereas a negative value indicates dispersion.

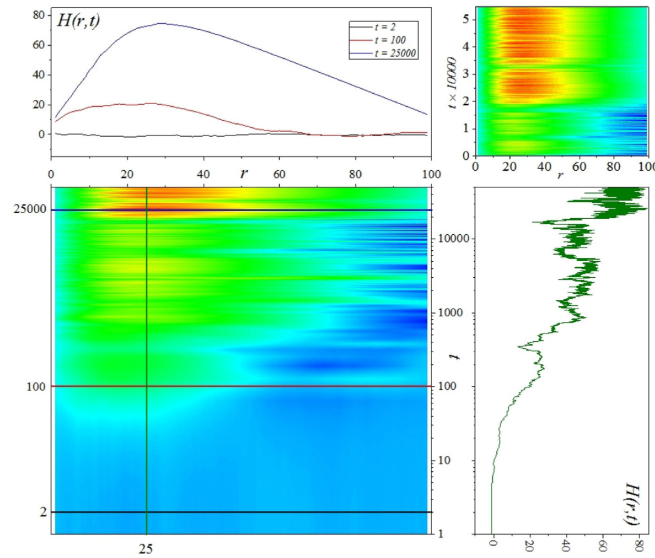


FIG. 7. The time dependence of the $H$ function. The bottom-left (top-right) panel is a color map of $H(r,t)$ in log (linear) scale. The top-left panel shows three profile plots $H(r,t)$ done along the horizontal lines shown in the bottom-left panel (for $t = 2$, 100, and 25 000). The bottom-right panel shows a profile of $H(r,t)$ done along the vertical line shown in the bottom-left panel (for $r = 25$). The parameters used are the same as in Fig. 5.

The value of $r$ that maximizes $H(r)$ indicates the radius of maximal aggregation.

In Fig. 7, we present a time evolution of $H(r,t)$. We begin our simulations from the uniformly distributed gliders. The initial condition is reflected by $H(r,0)$, visible as a flat black line in the top-left panel. Over the course of the simulation, the $H$ function becomes convex, having a maximum value of about $r_{\max} \approx 25$ (cf. red and blue lines in the top-left panel of Fig. 7), which seems to be the optimal cluster size that allows the gliders to use the available thermals most efficiently. For $t \approx 20\,000$, a single cluster composed of all $N_g$ gliders forms. Then, the cluster is stable for $t > 20\,000$, although from time to time it is disturbed due to some UAVs that temporarily lose contact with the flock (see the red area in the top-right panel in Fig. 7).

To verify how the optimal cluster size $r_{\max}$ is related to the density of thermals $\rho$, we have performed Ripley's statistics for different $\rho$ calculating

$$\hat{H}(r) = \left\langle \frac{1}{t_2 - t_1}\sum_{t=t_1}^{t_2} H(r,t)\right\rangle, \tag{10}$$

where the average is taken over 20 simulations beginning with different initial conditions. Times $t_1$ and $t_2$ are chosen so as to ensure the stationary behavior of the $H$ function and are $t_1 = 20\,000$ and $t_2 = 50\,000$ (see Fig. 7). Figure 8 presents the results of the analysis. The top panel shows that the maximal value of $\hat{H}(r)$ (marked by blue points) decreases with $\rho$, meaning that aggregation of gliders becomes less significant when the number of thermals increases. This is confirmed in the bottom panel, in which the $r$ position of this maximum (shown by black points) doubles from $r_{\max} \approx 17$ to $\approx 33$, indicating a

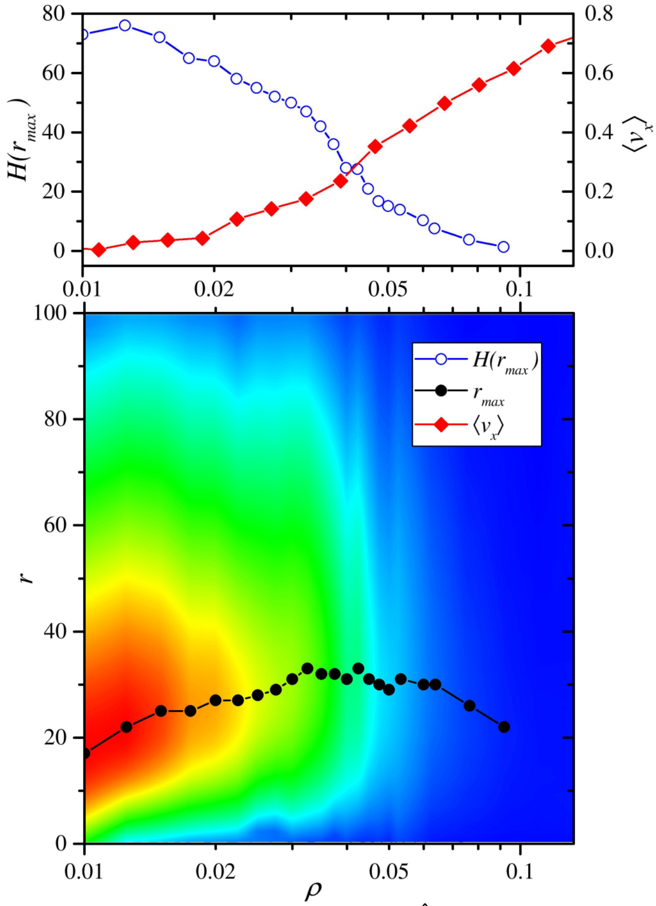


FIG. 8. The dependence of the average $\hat{H}$ function on the thermal density $\rho$ in the stationary regime [$H(r,t)$ is averaged over time for $20\,000 < t < 50\,000$]. Bottom panel: The color map of $\hat{H}(r)$. The black points mark the maximal value $r_{\max}$ of $\hat{H}(r)$ for a given $\rho$. Top panel: The blue open points represent the value $\hat{H}(r = r_{\max})$, and the red diamonds represent the dependence of the order parameter on $\rho$ (cf. red diamonds in Fig. 2). The parameters used are the same as in Fig. 5.

significant increase in the optimal cluster size. For $\rho > 0.05$, the behavior of $r_{\max}$ becomes meaningless, because the $H$ function flattens [cf. small values of $\hat{H}(r_{\max})$].

To visualize simultaneously the position of the critical density of thermals, the relationship of the order parameter on $\rho$ (red diamonds in the top panel of Fig. 8) has been reproduced from Fig. 2. It appears that the gliders cooperate only near the critical thermal's density. When the number of thermals is sufficient to enable a single glider to reach high speeds without the aid of the remaining UAVs, $H(r_{\max})$ decreases and the phenomenon of self-organization disappears. This is an intriguing observation that would mean, for example, that in the case of deteriorating weather conditions (a decreasing number of thermals), gliders would spontaneously organize themselves in clusters to survive unfavorable conditions. When the weather improved, the gliders would again spread over the entire area available.

## V. CONCLUSIONS

The self-organization of agents into a group, for example, birds into a flock, is a fairly simple phenomenon to achieve when appropriate rules are applied [17]. Usually, these rules act like forces that cause agents to keep close to other individuals. In evolutionary computation formalism, clustering can occur indirectly if it increases the fitness function of the algorithm. Both these approaches are well developed and understood. In this paper, we demonstrate that a flock can be formed in a completely different spontaneous way. This phenomenon is quite unexpected. After all, gliders are not rewarded for faster flight nor is their random exploration biased toward other gliders. It seems that the exchange of information pushes them into flight through narrow percolating paths of thermals in the same manner in which pressure forces water through a mesh sieve. As the number of thermals increases (analogous to a sieve's holes enlarging), the percolation paths (analogous to the flow of the water) become homogeneous.

It would be beneficial to reduce the glider model to a more abstract form, reducing the number of parameters but preserving the observed clustering, which would enable more in-depth examination of the causes of this phenomenon and possibly even enable its analytical description. This may be a focus of future research.

## ACKNOWLEDGMENT

This paper has been supported by the National Science Centre of Poland (Narodowe Centrum Nauki) under Grant No. 2012/05/E/ST2/02300.

[1] Circular No. 328 AN/190: Unmanned Aircraft Systems, ICAO, Retrieved 2 November 2017.

[2] D. Pack, R. Sward, S. Cooper, and G. York, Searching, detecting, monitoring, and tracking emergency sites using multiple unmanned aerial vehicles, in *Proceedings of the AIAA Infotech Aerospace Conference on Collaboration in UAV Systems, 2005* (unpublished).

[3] M. J. Allen, Updraft model for development of autonomous soaring uninhabited air vehicles, in *44th AIAA Aerospace Sciences Meeting and Exhibit, Aerospace Sciences Meetings* (AIAA, Reston, VA, 2006).

[4] J. W. Langelaan, Gust energy extraction for mini and micro uninhabited aerial vehicles, J. Guid. Control Dyn. **32**, 464 (2009).

[5] T. Guionnet, J. Martin, S. A. Shaffer, H. Weimerskirch, and D. P. Costa, Fast and fuel efficient optimal use of wind by flying albatrosses, Proc. R. Soc. B **267**, 1869 (2000).

[6] M. Allen and V. Lin, Guidance and control of an autonomous soaring vehicle with flight test results, in *45th AIAA Aerospace Sciences Meeting and Exhibit, Aerospace Sciences Meetings* (AIAA, Reston, VA, 2007).

[7] D. Edwards, Implementation details and flight test results of an autonomous soaring controller, in *AIAA Guidance, Navigation and Control Conference and Exhibit, Guidance, Navigation, and Control and Co-located Conferences* (AIAA, Reston, VA, 2008).

[8] P. Marqués and A. Da Ronch, *Advanced UAV Aerodynamics, Flight Stability and Control: Novel Concepts, Theory and Applications* (Wiley, New York, 2017).

[9] E. Amoiralis, M. Tsili, V. Spathopoulos, and A. Hatziefremidis, Energy efficiency optimization in UAVs: A review, Mater. Sci. Forum **792**, 281 (2014).

[10] P. DeLima and D. Pack, Maximizing search coverage using future path projection for cooperative multiple UAVs with limited communication ranges, in *Optimization and Cooperative Control Strategies*, edited by M. J. Hirsch, C. W. Commander, P. M. Pardalos, and R. Murphey, LNCIS Vol. 381 (Springer-Verlag, Berlin, 2009), pp. 103–117.

[11] M. J. Allen, Autonomous soaring for improved endurance of a small uninhabitated air vehicle, in *43rd AIAA Aerospace Sciences Meeting and Exhibit, Aerospace Sciences Meetings* (AIAA, Reston, VA, 2005).

[12] S. R. Broadbent and J. M. Hammersley, Percolation processes I: Crystals and mazes, Proc. Cambridge Philos. Soc. **53**, 629 (1957).

[13] N. Araújo, P. Grassberger, B. Kahng, K. J. Schrenk, and R. M. Ziff, Recent advances and open challenges in percolation, Eur. Phys. J. Spec. Top. **223**, 2307 (2014).

[14] E. N. Gilbert, Random plane networks, J. Soc. Ind. Appl. Math. **9**, 533 (1961).

[15] P. Bak, C. Tang, and K. Wiesenfeld, Self-Organized Criticality: An Explanation of the $1/f$ Noise, Phys. Rev. Lett. **59**, 381 (1987).

[16] A. Mogilner, L. Edelstein-Keshet, L. Bent, and A. Spiros, Mutual interactions, potentials, and individual distance in a social aggregation, J. Math. Biol. **47**, 353 (2003).

[17] T. Vicsek, A. Czirok, E. B. Jacob, I. Cohen, and O. Schochet, Novel Type of Phase Transitions in a System of Self-Driven Particles, Phys. Rev. Lett. **75**, 1226 (1995).

[18] H. Levine, W. J. Rappel, and I. Cohen, Self-organization in systems of self-propelled particles, Phys. Rev. E **63**, 017101 (2000).

[19] I. D. Couzin, J. Krause, R. James, G. D. Ruxton, and N. R. Franks, Collective memory and spatial sorting in animal groups, J. Theor. Biol. **218**, 1 (2002).

[20] M. Brambilla, E. Ferrante, M. Birattari, and M. Dorigo, Swarm robotics: A review from the swarm engineering perspective, Swarm Intell. **7**, 1 (2013).

[21] C. Antal, O. N. Granichin, and S. Levi, Adaptive autonomous soaring of multiple UAVs using simultaneous perturbation stochastic approximation, in *49th IEEE Conference on Decision and Control (CDC)* (IEEE, 2010), pp. 3656–3661.

[22] J. A. Cobano, D. Alejo, S. Vera, G. Heredia, S. Sukkarieh, and A. Ollero, Distributed thermal identification and exploitation for multiple soaring UAVs, in *Human Behavior Understanding in Networked Sensing*, edited by P. Spagnolo, P. Mazzeo, and C. Distante (Springer, New York, 2014).

[23] See Supplemental Material at http://link.aps.org/supplemental/10.1103/PhysRevE.97.032139 for movies.

[24] P. Balister, A. Sarkar, and B. Bollobás, Percolation, connectivity, coverage and colouring of random geometric graphs, in *Handbook of Large-Scale Random Networks*, edited by B. Bollobás, R. Kozma, and D. Miklós, Bolyai Society Mathematical Studies Vol. 18 (Springer, Berlin, Heidelberg, 2008), pp. 117–142.

[25] B. D. Ripley, The second-order analysis of stationary point processes, J. Appl. Probab. **13**, 255 (1976).

[26] G. Zhu, Y. Ge, and H. Wang, A modified Ripley's K function to detecting spatial pattern of urban system, in *21st International Conference on Geoinformatics, Kaifeng* (IEEE, 2013), pp. 1–5.

[27] P. Dixon, Ripley's K-function, in *Encyclopedia of Environmetrics*, edited by A. H. El-Shaarawi and W. W. Piergorsch (Wiley, New York, 2002), Vol. 3, pp. 1976–1803.

[28] M. A. Kiskowski, J. F. Hancock, and A. K. Kenworthy, On the use of Ripley's K-function and its derivatives to analyze domain size, Biophys. J. **97**, 1095 (2009).

[29] M. Jafari-Mamaghani, M. Andersson, and P. Krieger, Spatial point pattern analysis of neurons using Ripley's K-function in 3D, Front. Neuroinform. **4**, 9 (2010).